Title
Effects of charring on mass, organic carbon, and stable carbon isotope composition of wood

Journal
Organic Geochemistry, 33(11)

ISSN
0146-6380

Authors
Czimczik, Claudia I
Preston, Caroline M
Schmidt, Michael WI
et al.

Publication Date
2002-11-01

DOI
10.1016/s0146-6380(02)00137-7

Peer reviewed

PERGAMON

Organic Geochemistry 33 (2002) 1207–1223

Organic Geochemistry

www.elsevier.com/locate/orggeochem

Effects of charring on mass, organic carbon, and stable carbon isotope composition of wood

Claudia I. Czimczik[a,*], Caroline M. Preston[b], Michael W. I. Schmidt[c], Roland A. Werner[a], Ernst-Detlef Schulze[a]

[a]*Max-Planck-Institut fuer Biogeochemie, Postfach 100164, 07701 Jena, Germany*
[b]*Pacific Forestry Centre, Natural Resources Canada 506, West Burnside Road, Victoria, BC, Canada V8Z 1M5*
[c]*University Zurich, Department of Geography, Physical Geography, Biogeochemistry Group, Winterthurerstr. 190, 8057 Zurich, Switzerland*

Received 6 March 2002; accepted 14 August 2002
(returned to author for revision 30 May 2002)

Abstract

To aid in understanding black carbon (BC) formation during smoldering combustion in forest fires, we characterized charring of a softwood and hardwood. Charring (150, 340, 480 °C) caused mass loss (7–84%), enrichment of organic carbon (OC) (0–32%), and ^{13}C depletion (>150 °C). As determined by ^{13}C MAS NMR, the OC composition of the woods was dominated by (di)-*O*-alkyl structures, and the chars by alkyl and aromatic structures. With increasing temperature, aromatic structures increased and the chars became more similar, although initial differences in OC concentration and $\delta^{13}C$ of woods persisted. The BC cluster sizes apparently remained small, pointing towards a low resistance against oxidation.

1. Introduction

Current attempts to formulate ecosystem carbon budgets indicate a requirement for a very stable or even inert component of soil carbon (Falloon and Smith, 2000; Gleixner et al., 2002). The most likely candidate for this carbon pool is fire-derived black carbon (BC) (Kuhlbusch, 1998), which has been detected using a variety of chemical, microscopic, and spectroscopic techniques, including solid state carbon-13 nuclear magnetic resonance (^{13}C NMR) spectroscopy (Skjemstad et al., 1999; Schmidt and Noack, 2000). BC has recently been identified as a significant fraction in certain tropical (Glaser et al., 2001) and temperate soils (Skjemstad et al., 1996, 1999; Schmidt et al., 1999; Ponomarenko and Anderson, 2001). BC may also play an important role in carbon sequestration of boreal forest soils (Schulze et al., 1999; Turunen et al., 2001), where fire is a major disturbance (Harden et al., 2000; Amiro et al., 2001).

BC originates from two general sources (Schmidt and Noack, 2000): soot, with a highly-ordered structure results from condensation of small volatile particles in the gas phase of a fire, and char from incomplete combustion of solid wood in situ. The latter further comprises a variety of components since temperature and oxygen gradients exist within a burning log. Thus, BC may be expected to show a range of physical and chemical properties that may affect its long-term stability (Gleixner et al., 2001). BC represents a continuum of chemical and physical properties. The different methods used to analyze BC measure different parts of this continuum and can produce disparate results (Schmidt et al., 2001).

* Corresponding author. Tel.: +49-3641-643720; fax: +49-3641-643710.
E-mail address: czimczik@bgc-jena.mpg.de (C.I. Czimczik).

0146-6380/02/$ - see front matter
PII: S0146-6380(02)00137-7

A full understanding of the role of BC in global carbon cycling, and especially in fire-prone boreal forests will require a range of field, laboratory and modeling approaches. These include the detection of BC in organic and mineral soils, the characterization of its initial physical and chemical properties, and the understanding of its subsequent transport and transformation on a range of temporal and spatial scales. Surprisingly, there is little direct information on conversion rates of forest biomass to BC (Kuhlbusch et al., 1996; Bird et al., 1999; Tinker and Knight, 2000; Fearnside et al., 2001). Also, studies on the molecular structure and isotopic properties of char formed in forest wildfires do not exist.

While laboratory charring studies cannot simulate the full complexities of wildfire, they provide one avenue to understanding natural charring processes. Previous studies have included charring of individual wood components, such as cellulose (Shafizadeh, 1968; Pastorova et al., 1994; Sekiguchi et al., 1983; Banyasz et al., 2001; Völker and Rieckmann, 2002), pectin (Sharma et al., 2001), lignin (Oren et al., 1984), woody peat (Freitas et al., 1999), grass (Knicker et al., 1996) and rice hulls (Freitas et al., 2001). Only a few studies exist for wood charring (Solum et al., 1995; Baldock and Smernik, 2002).

To provide information relevant to charring of wood and BC formation in forest fires, we examined the influence of fire intensity, as a function of temperature and time, on the pattern of mass loss, organic carbon (OC) concentration and and $\delta^{13}C$ stable isotope ratio of wood and its major constituents (holocellulose and lignin) during laboratory charring. In nature, fires are very complex processes. BC mainly forms during flaming combustion (Kuhlbusch and Crutzen, 1995). However, BC also forms during smoldering combustion as it occurs in the inner part of burning logs during rapid surface fires or in peat fires. To mimic smoldering conditions and to enhance analytical reproducibility we selected pyrolytic charring conditions. We chose soft- and hardwood to investigate differences in charring and BC formation in coniferous and deciduous forests.

2. Material and methods

2.1. Sample origin

For wood sampling, we cut down a Scots pine (*Pinus sylvestris* L.) and a birch (*Betula pendula* ROTH) in a mixed forest stand in northwestern Germany (Neustadt a. Rbge, 52°30′N, 9°30′E), representing a coniferous softwood, and a deciduous hardwood, respectively. The woods were oven-dried (60 °C), finely ground in a ball mill (10 min), dried again, and stored in a desiccator.

The samples used to represent *holocellulose* and guaiacyl *lignin* were residues of white- and brown-rot, respectively from coastal forests of Vancouver Island, Canada. Highly-developed white-rot of larger-diameter logs (i.e. >12 cm) is unusual and the samples were not collected as part of a systematic study. The ^{13}C CPMAS NMR spectrum of the holocellulose 1 sample (Hemmingson) was previously published (Fig. 2e of Preston et al., 2000). The spectrum of holocellulose 2 (Cathedral Grove, unpublished) was similar, but with broader lines that could be caused by lower cellulose crystallinity, or higher hemicellulose content. The brown-rot samples, from a previous study of coarse woody debris (Preston et al., 1998), are typical of highly-decomposed logs of decay classes IV (lignin 1, sample 688) and V (lignin 2, 720). They could not be identified to species, but were most likely from Douglas fir (*Pseudotsuga menziesii* (MIRB.) FRANCO) or western red cedar (*Thuja plicata* DONN.). Their ^{13}C CPMAS NMR are shown in Fig. 5 of Preston et al. (1998). Lignin contents determined by ^{13}C CPMAS NMR were 99% (lignin 1) and 92% (lignin 2).

2.2. Pyrolyis/thermogravimetry

The effect of temperature on the thermal degradation of wood, holocellulose and lignin under pyrolytic conditions was studied by charring triplicate samples from 60 to 1000 °C in an argon atmosphere after drying to constant mass at 60 °C for 25 min. We chose pyrolytic conditions to mimic BC formation during combustion under oxygen-free conditions as they occur in the inner part of burning logs or peat fires (smoldering combustion). We chose a heating rate of 20 °C per minute as a compromise between time needed for a complete reaction at a temperature and the practical limits of the experiment time.

Charring was performed and changes in mass loss rates investigated using thermogravimetry (Mettler Toledo TGA/STDA851, Giessen, Germany; precision 1 μg; 5 scans per s).

Samples of 0.3 g were placed in 150 μl Al_2O_3 crucibles filled to one third of volume. Al_2O_3 powder served as a blank to correct for the decreasing buoyancy of the crucibles with increasing temperature of the argon atmosphere. To minimize air contact of the sample during inserting and to remove gases and aerosols evolving from the sample during charring, the oven environment of the thermogravimeter and the oven interior were permanently flushed with argon (80 or 20 ml per minute, respectively). From this experiment, we derived the temperature ranges where major changes in mass loss rates of the wood samples occurred: 150–340° and 340–480 °C.

To investigate the influence of charring time on mass loss within these temperature ranges, triplicates of both wood samples were isothermally heated at 150, 340, and 480 °C for 15 h (900 μl crucibles). The oven of the thermogravimeter was preheated at each temperature. After

isothermal charring, samples were stored in a desiccator. The accuracy of the thermogravimeter was tested by charring 30 mg of aluminum oxide (Al_2O_3), which is chemically and physically inert at the chosen temperatures. Again, Al_2O_3 also served as a blank. We tested the argon atmosphere for absence of oxidants by charring 30 mg of commercially available activated carbon, which would oxidize and thus decrease in mass if heated in the presence of oxygen. Both Al_2O_3 and activated carbon, were heated in 900 μl Al_2O_3 crucibles (360 °C, 15 h).

Sample mass was measured continuously during charring and recorded by the built-in software (Star 6.01) of the thermogravimetry apparatus.

Measurements of *organic carbon* (OC) concentrations and *stable carbon isotope ratios* ($\delta^{13}C$)[1] of dried and charred woods (chars) as well as post-run off-line calculation and evaluation for assigning the final $\delta^{13}C$ values on the V-PDB scale were performed as described by Werner and Brand (2001). In short, samples, laboratory reference material and blanks were combusted quantitatively using an elemental analyzer (NA 1110, CE Instruments, Rodano, Italy) coupled to a Delta^{plus} XL isotope ratio mass spectrometer (Finnigan MAT, Bremen, Germany) as described by Werner et al. (1999). The $\delta^{13}C$-values of the laboratory reference materials had been determined directly and compared with the international reference materials NBS22 oil ($\delta^{13}C = -29.78$ ‰$_{V\text{-}PDB}$) and USGS 24 graphite ($\delta^{13}C = -15.99$ ‰$_{V\text{-}PDB}$). The carbon content (% C) of the laboratory reference materials was calibrated versus a commercially available certificated standard material for elemental analysis (acetanilide; Merck, Darmstadt, Germany).

2.3. Solid state ^{13}C NMR spectra

Magic-angle spinning (MAS) data were obtained on finely-ground dried samples using a Bruker MSL 300 spectrometer (Bruker Instruments Inc., Karlsruhe, Germany) operating at 75.47 MHz. Wood samples were spun at 4.7 kHz in a 7 mm outer diameter rotor, and chars at 8.0 kHz in a 4 mm rotor. Cross-polarization (CP) spectra were acquired with 1 ms contact time, and 2257–8000 scans; the recycle time was 2.0 s for wood and 1.5 s for charred samples. CP spectra with dipolar dephasing (DD) were obtained with 46–47 μs dephasing time. This short delay period, without decoupling, is inserted between CP and signal acquisition. For the wood samples in the 7 mm rotor, dipolar dephasing was combined with the sequence for total suppression of spinning sidebands (SSB; TOSS), but this was not used for the char samples at higher spinning speed in the 4 mm rotor. In DD spectra, intensity is retained for carbon atoms without attached protons, and for those with some mobility in the solid state, such as acetate, methyl, and methoxy C, and methylene C in long chains.

The CP signal enhancement is reduced for carbon atoms that are remote from protons, have some mobility in the solid state, or are close to paramagnetic centers. Therefore, CPMAS spectra typically underrepresent amorphous long-chain CH_2 and the polycondensed structures of BC (Maroto-Valer et al., 1996; Skjemstad et al., 1999; Smernik and Oades, 2000; Freitas et al., 2001; Preston, 2001; Preston et al., 2002; Baldock and Smernik, 2002). To overcome this, we also obtained spectra using simple Bloch decay (BD) acquisition (without CP), with 720 scans and 100 s recycle time as determined to be sufficient for char samples by Smernik and Oades (2000) and Baldock and Smernik (2002). These were corrected for the spectrometer background (roughly equal to the magnitude of the signal with our equipment) by subtraction of the free-induction decay signal obtained from an empty rotor. To assess CP efficiency, a 720-scan CP spectrum was also obtained. The BD spectra have a lower signal-to-noise (S/N) ratio and resolution, but a quantitative intensity distribution. The CP and DD spectra, on the other hand, are useful for rapid acquisition and detailed examination of spectral features.

Spectra were processed with either the PC-based WinNMR, or the original Aspect DISMSL software (Bruker, Karlsruhe, Germany) using 40 Hz (CPMAS) or 60 Hz (DD, BD) line-broadening, with phasing and baseline correction under operator control. Chemical shifts are reported relative to tetramethylsilane (TMS) at 0 ppm, with the reference frequency set using the adamantane peak at 38.56 ppm.

2.4. Composition of fresh wood

The NMR spectra of wood samples were analyzed using the approach developed in Preston et al. (1998) and references therein. The spectra were divided into chemical shift regions, and the relative areas (expressed as percentages of total area—*relative intensity*) were used to estimate the percentage of C in carbohydrate, lignin, acetate, and "other" alkyl or carboxyl structures.

The alkyl region was divided into the intensities due to the acetate peak at 22 ppm, and other alkyl components. Methoxy C was the region from 50 to 58 ppm. The *O*-alkyl region was measured from 58 to 95 ppm, and the di-*O*-alkyl region from 95 to 112 ppm (softwood) or to 116 ppm (hardwood). The aromatic region extended from these boundaries to 153 ppm, the phenolic region to 160 ppm (softwood) or to 165 ppm

[1] Stable isotope abundances of elements are generally expressed as the relative difference of the isotope ratio of a compound to that of an international standard. The international standard for stable carbon isotope ratio measurements is: V–PDB = Vienna PeeDee Belemite with a $^{13}C/^{12}C$ ratio of $(11180.2 \pm 2.8)*10^{-6}$.

(hardwood), and the carboxyl region to 178 ppm (softwood) or to 185 ppm (hardwood). The 153–160 ppm region includes O- and N-substituted aromatic C. For wood, it is mainly the former, including both free phenolic groups, and aromatic ethers (–OCH_3). For convenience, we refer to it as "phenolic" in this paper. Corrections were made for SSB by assuming equal intensities for the upfield and downfield sidebands (Preston, 2001). For softwood, the carboxyl peak was small, and a SSB correction was not necessary. For hardwood, SSB corrections were made for aromatic, phenolic, and carboxyl regions.

The ratio of lignin, carbohydrate, and acetate monomer units was estimated using structural models of nine carbon atoms for the phenylpropane skeleton of lignin (Fig. 4), six carbon atoms for carbohydrate (hexose structure, Fig. 4), and two carbon atoms for acetate (CH_3–CO_2^-).

First, the intensity due to one lignin C was determined by attributing the aromatic plus phenolic region to six lignin carbon atoms for softwood and four for hardwood. The total intensity for lignin was then determined by multiplying the value for one lignin C by nine and adding the intensity due to methoxy C. Intensity due to carbohydrate was determined from the sum of the *O*- and di-*O*-alkyl C region, corrected for intensity from the 3-C side-chain of guaiacyl lignin, and additionally for hardwood, for the C2 and C6 of syringyl lignin. This was divided by 6 to get the intensity due to one carbohydrate C. The ratio of carbohydrate to lignin monomer units was determined from the ratio of the intensities for one carbohydrate C to one lignin C. The intensity due to acetate C was estimated by taking the value for acetate-methyl C at 22 ppm, and assuming an equal contribution for the carboxyl C of acetate. For other alkyl C, the intensity due to acetate was subtracted from that of the alkyl region. Other carboxyl C was the remainder of the carboxyl intensity after subtraction of the intensity due to acetate. Details of the calculations are shown with Table 2.

These calculations assume that hardwood contains only syringyl lignin, based on the relatively sharp phenolic peak at 153.5 ppm, and the very low intensity peak at 115–130 ppm. There is no compensation for underestimation of lignin in the CP spectra (Davis et al., 1994a; Preston et al., 1998). It is also assumed that carbohydrates are all based on a six-membered ring (hexose). However, this approach should be adequate to compare the bulk composition of the two wood samples.

2.5. Effects of charring

In contrast to the wood samples, the chars gave no distinct signals in the *O*-alkyl, di-*O*-alkyl and carbonyl regions, into which the broad aromatic signal extended. Therefore, the char spectra were only divided into alkyl and aromatic regions, with the boundary (typically around 80 ppm) determined by the minimum intensity (Solum et al., 2001). The areas were corrected for the SSB of the aromatic signal, by assuming equal intensity for both sidebands (Preston, 2001). The spinning speed of 8000 Hz was chosen as a compromise between reduction of SSBs vs. the loss of CP efficiency with increasing spinning speeds (Jakobsen et al., 1988). For intensity comparisons (CP vs. DD spectra with 8000 scans; CP vs. BD 720 scans) spectra were plotted in the absolute intensity mode using the Aspect computer. Difference (DIFF) spectra were obtained by subtraction of the DD from the CP spectra, retaining the absolute intensity setting.

3. Results

3.1. Mass loss

Loss from softwood and hardwood during charring from 60 to 1000 °C followed similar patterns. Major changes in mass occurred within two temperature intervals, from 150 to 340 and 340 to 480 °C (Fig. 1a). Total mass loss at 1000 °C was 85% of initial mass for softwood and 91% for hardwood.

The mass loss pattern of holocellulose samples differed from those of the wood samples. The two holocellulose samples also differed in their (i) mass loss pattern, (ii) maximum mass loss, and (iii) the temperature at which highest mass loss occurred (Fig. 1b). Highest mass loss occurred between 345 and 365 °C and total mass loss at 1000 °C was 86–92% of initial mass. Lignin samples also differed from the wood samples in their mass loss pattern, but both lignin samples followed a similar pattern. Mass loss was lower than that of wood or holocellulose, and did not show distinct temperature ranges associated with high mass loss (Fig. 1c). Total mass loss at 1000 °C was 63–65% of initial mass. The mass loss patterns of holocellulose and lignin samples combined did not reflect those of the wood samples.

We continuously monitored the mass of the two wood samples during isothermal charring at 150, 340, and 480 °C in the absence of oxygen. Constancy of mass was defined as variations of <0.01 mass-% per minute, which was the maximum mass loss of the blank Al_2O_3. Mass loss of activated carbon did not exceed blank variation, suggesting the absence of reactive, e.g. oxygen-containing, compounds during sample insertion and charring in the thermogravimetry oven.

Two trends became evident. First, mass loss of all samples was highest within the first 10 min and then leveled off asymptotically (Fig. 2). Within the first 10 min, samples lost on average 6% (150 °C), 40% (340 °C), and 81% (480 °C) of their initial mass (60 °C), compared to 7% (150 °C), 54% (340 °C), and 84% (480 °C) after 15 h. The standard deviation among

replicates was higher for softwood than for hardwood at each temperature. The masses of both wood samples stabilized at each temperature within 15 h and no trend was found between temperature and time needed to reach constant mass. Second, compared to the initial dry mass, the mass of wood samples decreased with increasing charring temperature (Table 1), with the highest mass loss occurring between 150 and 340 °C.

The mass loss of wood samples was similar between 60 and 150 °C, but the mass loss of softwood was smaller than of hardwood during charring at higher temperatures.

3.2. Organic carbon

After charring at 150 °C, the organic carbon (OC) concentrations of both chars did not differ from the initial OC concentrations of both wood samples (Table 1). Charring at higher temperatures increased OC concentrations of the chars by 50% (340 °C) and 60% (480 °C) compared to wood samples. At each temperature, the softwood char had higher OC concentrations than the hardwood char.

For both samples, the volatiles emitted per temperature step were dominated by OC (50–71%) between 60 and 150 °C and 340 and 480 °C, respectively, but OC accounted for only 24% between 150 and 340 °C. The OC fraction of the volatiles was higher for softwood than for hardwood between 60 and 150 °C, and 340 and 480 °C, but lower between 150 and 340 °C.

3.3. Stable carbon isotope composition

During charring at 150 °C, $\delta^{13}C$ values of both chars became more positive (enriched in ^{13}C) (Table 1). In contrast, at higher temperatures $\delta^{13}C$ values became more negative, by 0.5–0.8 and 0.6–1.1‰ at 340 and 480 °C, respectively. At each temperature, the softwood (wood and chars) was depleted in ^{13}C compared to the hardwood.

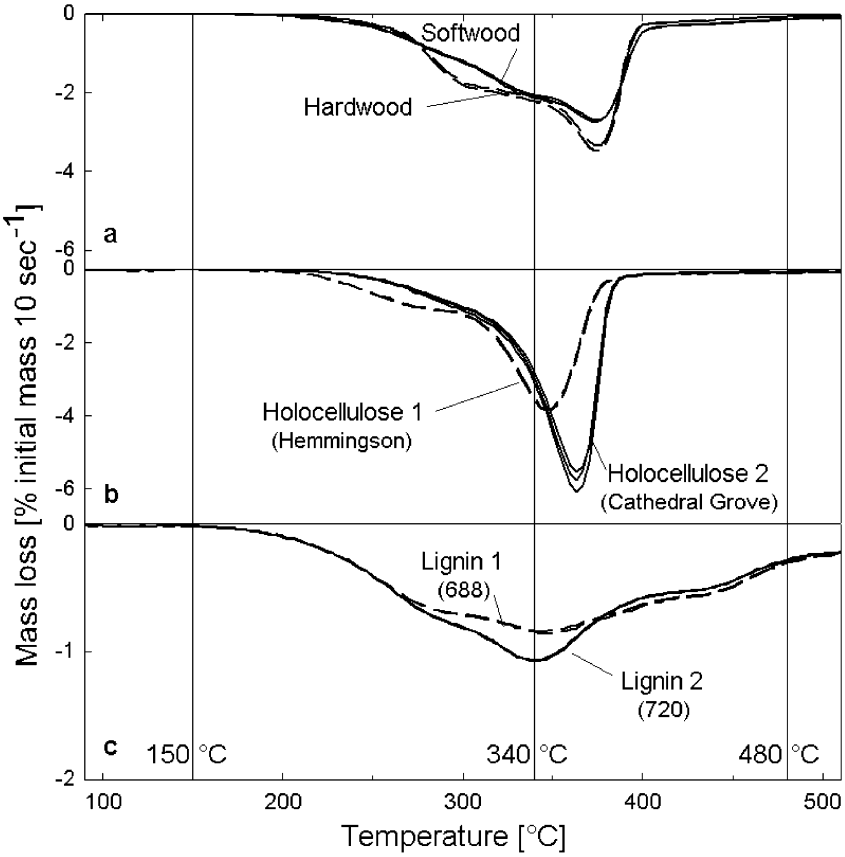

Fig. 1. Rate of mass loss of (a) softwood (*Pinus sylvestris* L.) and hardwood (*Betula pendula* Roth) and (b) two holocelluloses (natural white-rot), and (c) guaiacyl lignins (natural brown-rot) during charring in an argon atmosphere with a heating rate of 20 °C per minute using thermogravimetry. Samples were run in triplicate. Please note the different scale for (c).

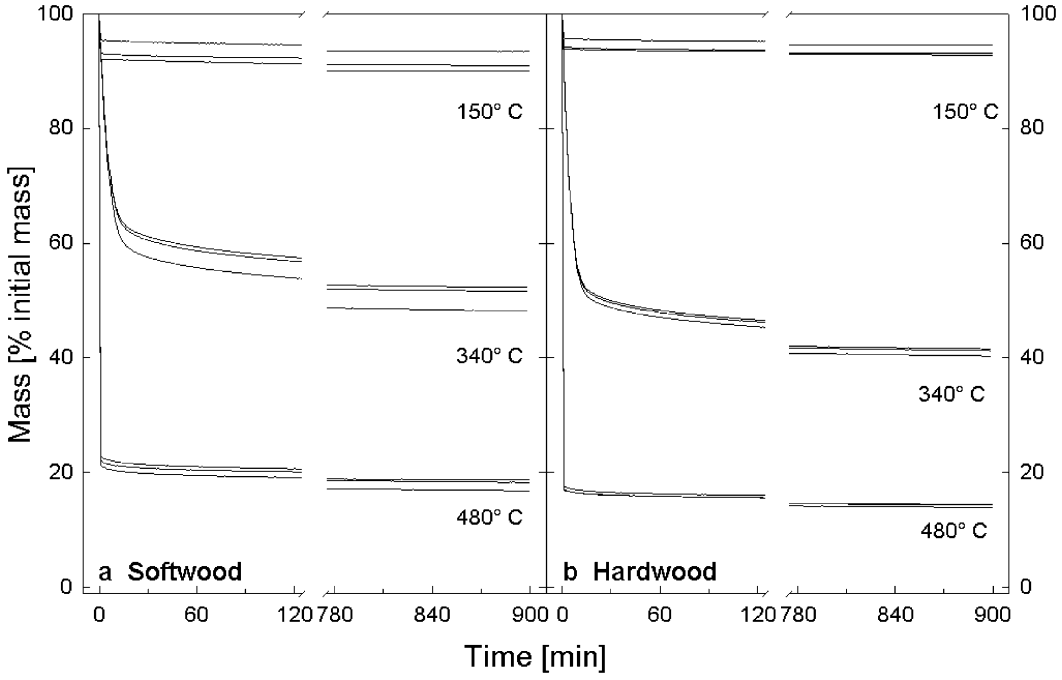

Fig. 2. Mass of (a) softwood (*Pinus sylvestris* L.) and (b) hardwood (*Betula pendula* Roth) during isothermal charring at 150, 340 or 480 °C in an argon atmosphere for 15 h using thermogravimetry. Please note the discontinuities of *x*-axes.

Table 1
Mass, organic carbon concentration, and stable carbon isotope values of softwood (*Pinus sylvestris* L.) and hardwood (*Betula pendula* Roth) after drying (60 °C) and charring at 150, 340 and 480 °C for 15 h in an argon atmosphere (±indicates standard deviation)

Residue (wood 60 °C, chars 150–480 °C)				Volatiles per temperature step (calculated)			
Temperature (°C)	Mass (% initial mass)	Organic carbon concentration (g C kg^{-1} residue)	Isotope composition ($\delta^{13}C$)[a] (‰ vs. V-PDB)	Temperature step (°C)	Mass (% mass of starting temperature)	Organic carbon concentration[b] (g C kg^{-1} volatiles)	Isotope composition ($\delta^{13}C$)[a,c] (‰ vs. V-PDB)
Softwood							
60	100.0	510±7	−29.4±0.0				
150	92±2	508±4	−29.1±0.2	60 to 150	8	533	−32.7
340	51±2	789±31	−30.2±0.2	150 to 340	41	158	−22.3
480	18±1	833±9	−30.5±0.0	340 to 480	33	765	−30.0
Hardwood							
60	100.0	484±4	−28.2±0.1				
150	94±1	484±1	−27.9±0.1	60 to 150	6	484	−32.9
340	41±1	704±18	−28.7±0.1	150 to 340	53	314	−26.5
480	14±0	790±10	−28.8±0.1	340 to 480	27	659	−28.6

[a] $\delta^{13}C\ [‰]_{V\text{-}PDB} = \left[\frac{(^{13}C/^{12}C)_{Sample}}{(^{13}C/^{12}C)_{V\text{-}PDB}} - 1\right] * 1000$

[b] $OC_{volatiles} = ((mass*OC_{residue\ at\ lower\ temperature}) - (mass*OC_{residue\ at\ higher\ temperature}))/mass_{volatiles}$.

[c] $\delta^{13}C_{volatiles} = ((mass*OC*\delta^{13}C_{residue\ at\ lower\ temperature}) - (mass*OC*\delta^{13}C_{residue\ at\ higher\ temperature}))/mass*OC_{volatiles}$.

OC emitted as volatiles from both wood samples between 60 and 150 °C was depleted in ^{13}C compared to the wood samples with similar $\delta^{13}C$ values for both woods. OC emitted between 150 and 340 °C was enriched compared to the 150 °C chars, with OC in volatiles from softwood being more enriched than from hardwood. OC emitted between 340° and 480 °C had a similar $\delta^{13}C$ value as the 340 °C chars.

3.4. Composition of wood

The NMR spectra for wood (Fig. 3) are dominated by peaks in the di-*O*- and *O*-alkyl region due to holocellulose (cellulose plus hemicellulose, Fig. 4) (Kolodziejski et al., 1982; Davis et al., 1994a, b; Preston et al., 1998). Both spectra have a peak for the methoxy C of lignin at 56 ppm. In the aromatic region, the softwood spectrum is typical of guaiacyl lignin (Fig. 4). In contrast, the pattern for hardwood is characteristic of syringyl lignin (Fig. 4) (Davis et al., 1994b; Solum et al., 1995). Both wood samples had low signal intensities in the alkyl region. The signal intensity for non-acetate alkyl C was greater for softwood, while acetate (22 ppm) and carboxyl (172 ppm) peaks were more prominent for hardwood.

The qualitative DD-TOSS spectra are consistent with these trends. Compared to the aromatic and phenolic peaks, the carboxyl, methoxy and acetate peaks are smaller for softwood than for hardwood. However, in addition to its weak acetate peak, softwood has a broad, weak signal due to methyl and alkyl carbon from approximately 12–38 ppm. For both spectra, the methoxy peak at 56 ppm has a broad shoulder at 62–70 ppm. This may be because the C6 of carbohydrates, a CH_2OH group, has greater mobility than the ring carbons, and thus loses intensity more slowly in the dephasing experiment (Newman et al., 1996).

The composition estimates (Table 2) show that the softwood is higher in lignin and alkyl carbon, but lower in acetate than the hardwood. The ratio of carbohydrate to lignin monomer units was 20% lower for softwood than for hardwood. The number of methoxy units per lignin aromatic ring was 50% lower for softwood than for hardwood, and for both woods 75–80% lower than the values of pure guaiacyl and syringyl monomers. The hardwood probably contains some guaiacyl units, while for both spectra, the area of the methoxy signal is poorly resolved from the much larger *O*-alkyl regions. The higher proportion of lignin C in softwood is consistent with its 3% higher OC concentration (Table 1).

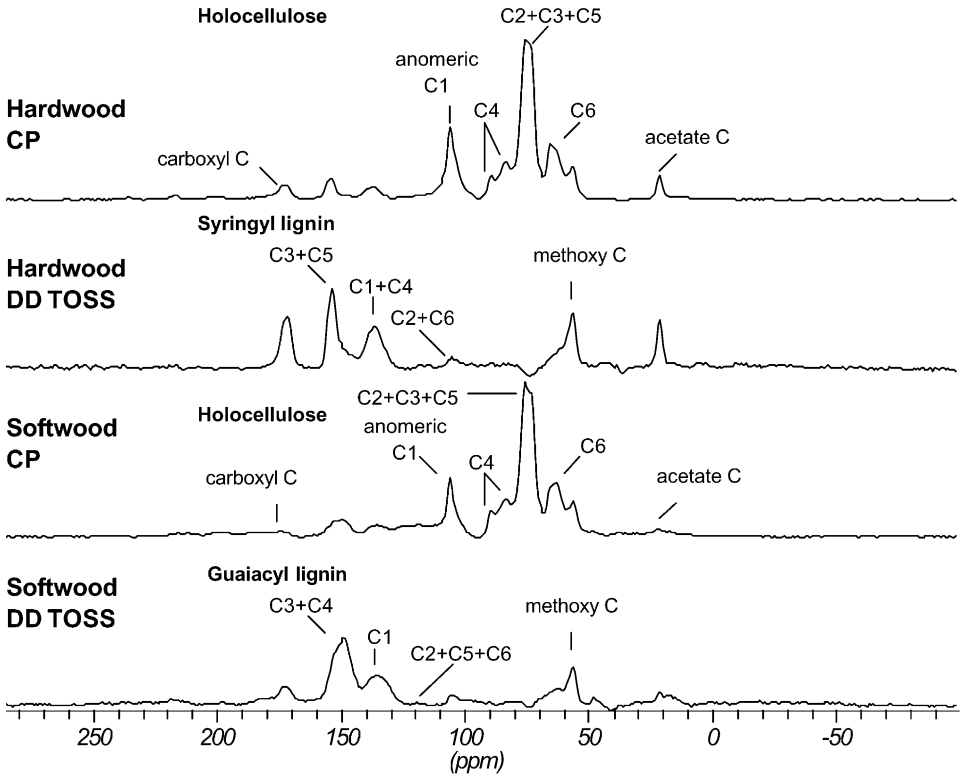

Fig. 3. ^{13}C CPMAS and dipolar-dephasing with total suppression of spinning sidebands (DD TOSS) NMR spectra of softwood (*Pinus sylvestris* L.) and hardwood (*Betula pendula* Roth), both dried at 60 °C.

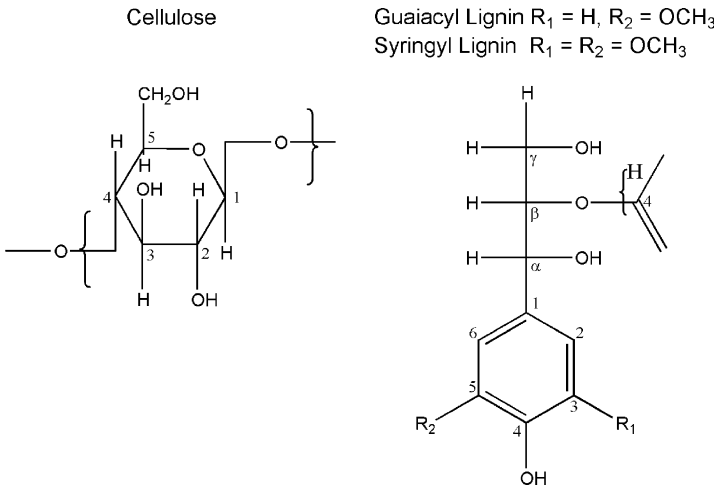

Fig. 4. Partial structures of wood carbohydrates and lignins. Carbohydrates form holocellulose, a mixture of cellulose (linear chains of β-1,4-bonded D-glucose) and hemicelluloses (linear and non-linear chains of hexose and pentose units). Guaiacyl lignin of softwood mainly consists of coniferyl alcohol. In our study, hardwood mainly contained syringyl lignin which is based on sinapyl alcohol. In lignin polymers, these phenylpropanoids are linked via ether (mainly 8-*O*-4′) or C–C bonds.

Table 2
Calculated composition of softwood (*Pinus sylvestris* L.) and hardwood (*Betula pendula* ROTH) after drying (60 °C) as revealed by solid-state ^{13}C CPMAS NMR spectroscopy

Region	Softwood	Hardwood
	% total organic carbon	
Acetate-methyl C	2.0	3.0
Other alkyl C	3.2	1.2
Total alkyl (0–50 ppm)	5.2	4.1
Methoxy C	3.4	5.7
O-alkyl C	50.9	55.8
Di-O-alkyl C	11.7	14.3
Aromatic C	18.9	8.1
Phenolic C	7.7	6.8
Carboxyl C	2.2	5.3
Derived structural parameters[a]		
Lignin	43.3[b]	39.2[c]
Carbohydrate	49.3[d]	51.5[e]
Acetate[f]	4.0	5.9
Other alkyl (= total alkyl- acetate-methyl)	3.2	1.1
Other carboxyl (= carboxyl- acetate-methyl)	0.2	2.3
Carbohydrate/lignin monomers	1.9	2.3
Methoxy/lignin monomers	0.8	1.5

[a] The ratio of carbohydrate, lignin and acetate monomer units was estimated using the single-carbon intensity based on structural models of six carbons for carbohydrate, nine for lignin (i. e. methoxy C was not used to estimate relative proportions of monomer units, but included in the percentage of total lignin C), and two for acetate.

[b] Aromatic + phenolic = 18.9 + 7.7 = 26.6% (6C), lignin monomer = 26.6/6C = 4.4%, total lignin = 9 lignin monomers + methoxy C = 43.30%.

[c] Aromatic + phenolic = 14.9% (4C), lignin monomer = 3.7%, total lignin = 9 lignin monomers + methoxy C = 39.18%.

[d] *O*- + di-*O*-alkyl (50.9 + 11.7) - 3C side-chain of guaiacyl lignin (3 lignin monomers = 3 * 4.4) = 49.26, carbohydrate monomer = 49.26/6C = 8.2%.

[e] *O*- + di-*O*-alkyl (70.1%) - 5 lignin monomers (5 * 3.7%) = 51.49%, with *O*-alkyl region corrected for 3C side-chain of guaiacyl lignin (3 monomers), and di-*O*-alkyl for C2 and C6 of syringyl lignin (2 monomers), carbohydrate monomer = 51.49/6C = 8.6%.

[f] Acetate-methyl C + equal contribution for the carboxyl C of acetate (2C).

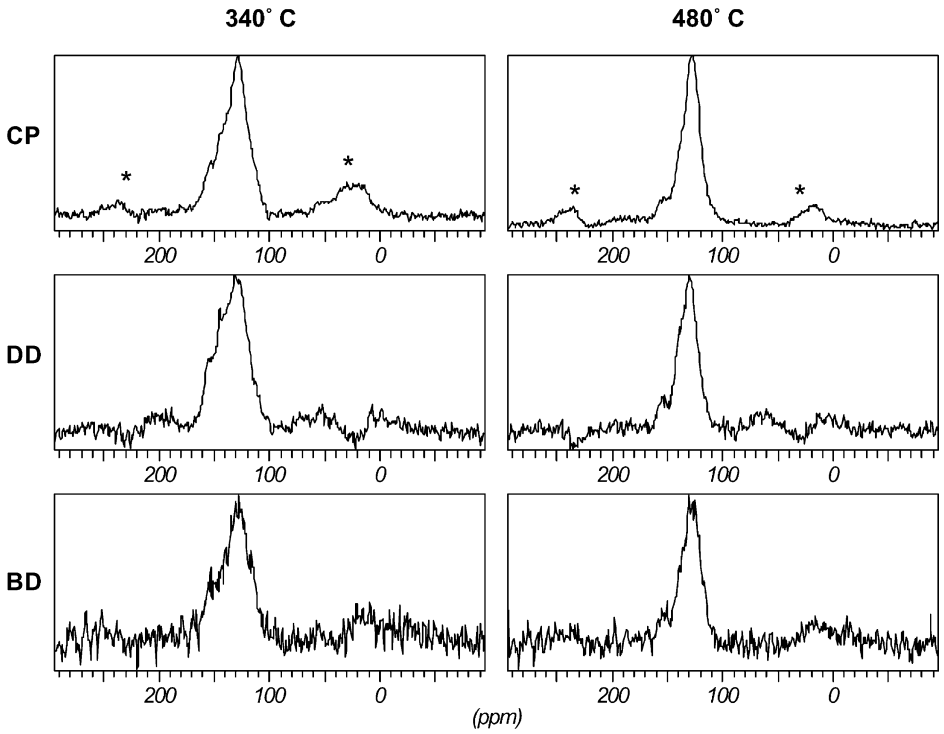

Fig. 5. ^{13}C NMR CPMAS, dipolar-dephasing (DD), and Bloch decay (BD) spectra of softwood (*Pinus sylvestris* L.), isothermally charred at 340 and 480 °C in an argon atmosphere for 15 h. Spinning sidebands are indicated as *.

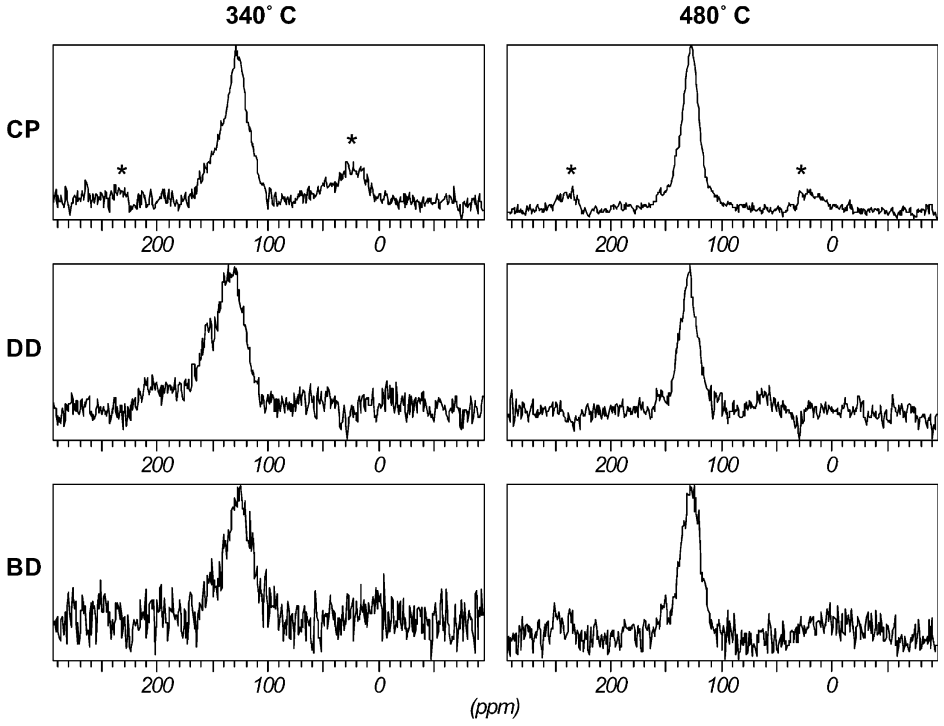

Fig. 6. ^{13}C NMR CPMAS, dipolar-dephasing (DD), and Bloch decay (BD) spectra of hardwood (*Betula pendula* Roth), isothermally charred at 340 and 480 °C in an argon atmosphere for 15 h. Spinning sidebands are indicated as *.

Table 3
Molecular structural composition of softwood (*Pinus sylvestris* L.) and hardwood (*Betula pendula* Roth) after drying (60 °C) and charring at 340 and 480 °C for 15 h in an argon atmosphere as revealed by solid-state ^{13}C CPMAS NMR spectroscopy

Temperature (°C)	DD/CP aromatic C[a]	CP/BD total integral[b]	Chemical shift region (^{13}C)[c] (relative intensity [% total area])					Technique
			carboxyl aromatic + phenolic		di-*O*-alkyl	*O*-alkyl	alkyl	
Softwood								
60	–	–	2	27	12	54	5	CP
340	0.60	0.42	–	84	–	–	16	CP
	–	–	–	92	–	–	8	BD
480	0.42	0.43	–	96	–	–	4	CP
	–	–	–	93	–	–	7	BD
Hardwood								
60	–	–	5	15	14	61	4	CP
340	0.80	0.44	–	80	–	–	20	CP
	–	–	–	91	–	–	9	BD
480	0.30	0.49	–	97	–	–	3	CP
	–	–	–	96	–	–	4	BD

[a] 112–153 ppm (softwood) or 116–153 ppm (hardwood), 8000 scans.
[b] 0–250 ppm, 720 scans.
[c] At 60 °C: alkyl 0–58 ppm, *O*–alkyl 58–95 ppm, di–*O*–alkyl 95–112 ppm (softwood) or 95–116 ppm (hardwood), aromatic + phenolic 112–160 ppm (softwood) or 116–165 ppm (hardwood), carbonyl 160–178 ppm (softwood) or 165–185 ppm (hardwood), at 340° and 480 °C in ppm: alkyl 0–80 ppm, aromatic + phenolic 80–185 ppm.

3.5. Effects of charring

Both wood samples showed similar changes in their CP spectra during isothermal charring (Figs. 5 and 6). Chars produced at 340 and 480 °C had low alkyl and high aromatic intensity, with loss of the *O*-alkyl and di-*O*-alkyl structures that dominated the initial wood (Table 3). The higher charring temperature (480 °C) resulted in a further increase of aromatic and decrease of alkyl C, and a similar intensity distribution for both chars as determined by both BD and CP techniques.

The assignment of peaks in the char spectra is based on studies of coal (Sullivan and Maciel, 1982; Wilson et al., 1984; Hu et al., 2001), cokes and catalyst chars (Fonseca et al., 1996b; Maroto-Valer et al., 1996, 1998) and soot (Solum et al., 2001). For all four chars, the alkyl C signal was broad, weak, and distorted by the upfield SSB of the aromatic region centered at 20–21 ppm at 8000 Hz MAS. After subtraction of the SSB intensity, all samples still had some alkyl intensity as shown in Table 3. The position of the poorly-defined peak maximum was estimated at 28–29 ppm, slightly offset from that of the SSB. The alkyl signal probably arises from a combination of methylene C in short chains or bridging groups, and methyl groups, including those directly bonded to aromatic C at 22 ppm.

The aromatic peak maximum was at 126–127 ppm, except for the hardwood 340 °C char where it was broader (125–129 ppm). The peak was asymmetric, with a shoulder for phenolic C at 152–155 ppm, and a weaker feature for C-substituted aromatic C at 140 ppm. For the hardwood 340 °C char the phenolic intensity was represented only as unresolved asymmetry of the much larger aromatic signal. The absence of a methoxyl peak in all char samples, in contrast to wood, indicated that the phenolic intensity arose mainly from phenolic –OH, without a contribution from aromatic $–OCH_3$. Despite the poor resolution of these features, comparison of the 340° and 480 °C char spectra indicated a loss of phenolic vs. aromatic intensity at the higher charring temperature, resulting in a narrower and more symmetric aromatic signal. This narrowing was also consistent with loss of C-substituted aromatic C around 130–145 ppm, and the associated loss of alkyl intensity.

The DD spectra were also dominated by the aromatic signal, with very low alkyl intensity (Figs. 5 and 6). It was difficult to quantify the intensity, or even to specify the chemical shifts, in the alkyl region of the DD spectra with any confidence. Even in the normal CP spectra, the alkyl signal was very broad and weak, and in the DD spectra it seemed to be further distorted by phase inversion of the broad SSB of the aromatic signal. A similar effect was noted by Wilson et al. (1984), although at longer dephasing times. Qualitatively, the DD spectra indicated very low or non-detectable levels of quaternary alkyl C, or of mobile methyl or methylene C.

For the DD spectra, the aromatic peak maximum was at 130–131 ppm for softwood, slightly higher than for the CP spectra (126–127 ppm). For the hardwood, there was less of a difference, with the maxima occurring at

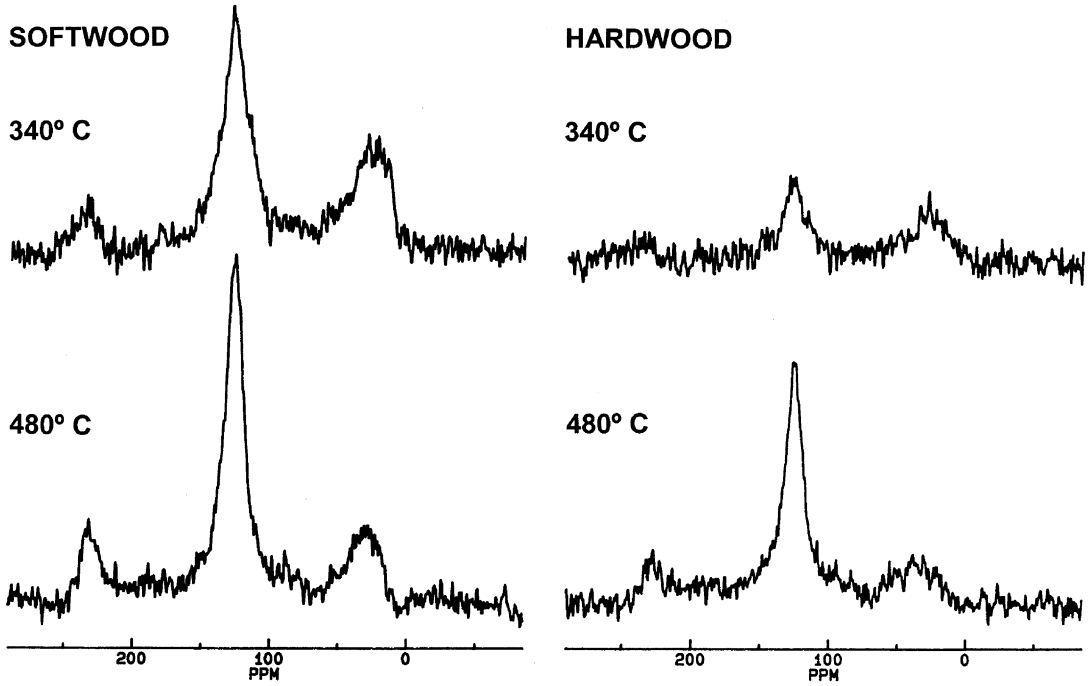

Fig. 7. Difference spectra of ^{13}C NMR CPMAS and dipolar-dephasing with 8000 scans of softwood (*Pinus sylvestris* L.) and hardwood (*Betula pendula* Roth), isothermally charred at 340 and 480 °C in an argon atmosphere for 15 h. Spinning sidebands are indicated as *.

128 ppm (340 °C) and 129 ppm (480 °C). The phenolic shoulder was better resolved in the DD spectra, due to its slightly slower rate of signal loss, especially for the softwood 340 °C char which had peaks at 145 and 155 ppm. The DD spectra also indicated lower phenolic intensity with increasing temperature leading to a more symmetric aromatic peak. The integrals for the aromatic region showed 0.30–0.80 of signal remaining after the 46–47 μs dephasing period, with greater signal loss for the higher-temperature (480 °C) chars (Table 3).

Difference spectra showing protonated C were generated by subtracting the DD from the CP spectra (Fig. 7). These had a well-defined alkyl region, similar to that seen in the normal CP spectra, and a more symmetric aromatic peak at 128–129 ppm (340 °C) and 125–126 ppm (480 °C). A similar pattern was seen in CP, DD, and difference spectra for coke deposits (Netzel et al., 1996).

3.6. CP efficiency and NMR visibility for chars

The BD spectra with 720 scans (shown in Figs. 5 and 6) had the same general features as the CP spectra, with lower signal-to-noise ratios, but a higher proportion of aromatic C. Compared to the BD technique, the CP spectra resulted in an underestimation of aromatic C and overestimation of alkyl C for the 340 °C samples (Table 3). At 480 °C, however, both techniques gave similar intensity distributions. Direct comparison of BD and CP spectra obtained with 720 scans (720-scan CP spectra not shown) showed low CP efficiency with total integrated intensity of the CP spectra only 0.42–0.49 of the corresponding BD spectra (Table 3).

4. Discussion

4.1. Mass loss

The similar trends of mass loss for softwood and hardwood during charring, with two temperature intervals of major changes, could not be easily explained by the mass loss patterns of holocellulose and lignin, the major components of wood, as proposed by Wiedemann et al. (1988). However, our results are in line with previous findings by Susott (1982), that mass loss pattern, and thus thermal stability, of wood seems to be mainly controlled by its cellulose and less by its lignin content and structure. During charring, cellulose undergoes thermal degradation (dehydration and fragmentation) to volatiles (mainly CO, CO_2, and H_2O) and tar (mainly levoglucosan) that can further undergo condensation reactions to form alkyl and aromatic C (BC) (Shafizadeh, 1968, 1982; Sekiguchi et al., 1983; Shafizadeh and Sekiguchi, 1983; Banyasz et al., 2001; Elias et al., 2001).

Our results showed that both wood samples had their highest mass loss in the same temperature range as both holocellulose samples (340–480 °C). The higher rate of mass loss for hardwood below 340 °C may be explained by its different structure compared to holocellulose. This assumption is based on ^{13}C CPMAS NMR spectra of holocellulose 1 that had either a higher cellulose content or a larger cellulose crystallite size compared to holocellulose 2, showing a greater splitting of the double peak at 73–75 ppm (C2, C3, and C5), a higher ratio of 66–63 ppm (C6), a lower ratio of 89–83 ppm (C4), and a more symmetric peak at 105 ppm (anomeric C1) (unpublished results). Further, mass loss below 340 °C may be due to the loss of gaseous hydrocarbons (volatile monoterpenes) and nongaseous hydrocarbons (condensed resin and fatty acids, and their esters, sequiterpenoid compounds) (Susott, 1980; McGraw et al., 1999). Thus, using thermogravimetry it was possible to distinguish the two holocellulose samples.

The lignin samples did not decompose in a single main temperature range, but showed a very low mass loss rate over the entire range between 200 and 400 °C. During pyrolysis, lignin mainly undergoes cleavage of the β-*O*-C4 aryl ether linkage (Britt et al., 2000), while the aromatic ring of lignin (methoxy phenyl groups) mainly resists thermal degradation under pyrolytic conditions (Sekiguchi et al., 1983; González-Vila et al., 2001) and acts as a precursor for BC (Oren et al., 1984). The lower rate of mass loss for lignin 1 at all temperatures may be explained by its higher lignin content compared to lignin 2 which was chemically less decomposed.

Increasing mass loss with temperature is typical for isothermal charring and analytical pyrolysis (Schnitzer and Hoffman, 1965; Drysdale, 1999; Schleser et al., 1999; Sharma et al., 2001). Mackay and Roberts (1982) found a higher char yield from wood charring (30%) which may be explained by trapping of tar (e.g. levoglucosan) during charring, that would lead to a lower mass loss and higher char yield (Antal et al., 1996). Tar trapping was not an important process in this study, due to the low sample mass and constant flushing of the oven interior. Thus, lignin samples could be distinguished by thermogravimetry.

The smaller mass loss of softwood compared to hardwood can be explained by its lower cellulose and higher lignin content (Mackay and Roberts, 1982; Susott, 1982; Shafizadeh, 1982; Sekiguchi et al., 1983; Jakab et al., 1997). Further, mass loss of woods may be affected by differences in ash content and composition (Mingle and Boubel, 1968; Shafizadeh and Sekiguchi, 1983; Jakab et al., 1997) and initial bulk density (Völker and Rieckmann, 2002).

Higher variation in mass loss of softwood may be explained by differences in the particle structure after grinding. Softwood, with a softer physical structure than hardwood, produced larger, and thus more heterogeneous particles than hardwood and this affects the charring process in thermogravimetry.

4.2. OC concentration

The OC concentration of our wood samples was typical for biomass (40–50 mass-%). The higher OC concentration of softwood 340 °C char and the higher OC concentration of softwood volatiles, emitted during charring between 150 and 340 °C, can be explained with the lower cellulose and higher lignin content of softwood compared to hardwood, since cellulose contains less OC than lignin and is preferentially lost within this temperature region (see earlier).

During thermal treatment, OC concentrations of both wood samples increased with increasing temperature, while mass decreased. This is consistent with a decrease in the O/C and H/C ratios (Shafizadeh and Sekiguchi, 1983; Kuhlbusch, 1995; Schleser et al., 1999). The higher OC concentration of softwood at all temperatures may be explained by its initially higher OC concentration (Mackay and Roberts, 1982).

4.3. Stable isotope composition

Plants are depleted in ^{13}C relative to atmospheric CO_2. The $\delta^{13}C$ value of CO_2 from ambient air is derived from respiration processes of plants and soils and background atmosphere. This ^{13}C depletion relative to CO_2 is caused during photosynthesis by isotope fractionations principally associated with diffusion of CO_2 through the stomata into the intercellular system and carboxylation (CO_2-fixation) with minor contributions from other factors. The isotope fractionation varies as the relative resistivities of stomatal diffusion and carboxylation varies. Parameters influencing this isotope fractionation are the photosynthetic pathway, ambient light intensity, temperature, humidity, and (soil) water availability. $\delta^{13}C$ values of the investigated wood samples were within the typical range for C3 plants (Ehleringer et al., 2000).

In this study, the ^{13}C depletion of bulk softwood compared to hardwood can mainly be explained by its lower cellulose and higher lignin content. Cellulose is enriched in ^{13}C by 1–2 ‰, whereas lignin is lighter by 4–7 ‰ than bulk wood (Benner et al., 1987; Ehleringer et al., 2000). Other factors contributing to the $\delta^{13}C$ of wood such as differences in water use efficiency, which would lead to a ^{13}C enrichment of bulk softwood compared to hardwood (Brugnoli et al., 1998), and growing conditions (Broadmeadow and Griffith, 1993), which were similar in this study for both woods, should be of minor importance here.

The preservation of the difference in the $\delta^{13}C$ values between softwood and hardwood found in this study, corresponds with findings from Schleser et al. (1999) for

the thermal degradation of wood, and Turekian et al. (1998), who measured a small ^{13}C enrichment (+0.5 ‰) in aerosol particles from smoldering combustion of C3 plants.

Our theory of volatilization of gaseous and nongaseous hydrocarbons between 60 and 150 °C is supported by the $\delta^{13}C$ values of the corresponding fractions (Table 1). The volatilized fractions of both wood types show a depletion in ^{13}C ($\Delta\delta^{13}C$ −3.3 to −4.7 ‰) relative to total wood. Lipids are known to be ^{13}C depleted relative to carbohydrates (O'Malley et al., 1997). The kinetic carbon isotope effect of the pyruvate dehydrogenase reaction is responsible for this relative ^{13}C depletion of lipids synthesized from acetate units (Melzer and Schmidt, 1987). The OC concentration of these fractions however equals the OC concentration of bulk wood. This hints of simultaneous volatilization of products with very low or no carbon content, probably H_2O.

It is interesting to note that the volatiles of both woods emitted between 60 and 150 °C showed the same $\delta^{13}C$ values, although both woods probably differed in their content and composition of gaseous hydrocarbons and nongaseous hydrocarbons.

The subsequent ^{13}C depletion during charring at 340 °C is mainly due to the loss of (isotopically heavier) cellulose and is therefore smaller for softwood (containing less cellulose and more lignin) than hardwood. Further, methoxy C from the degradation of lignin may contribute to the depletion. Due to further kinetic isotope effects in the secondary metabolism of plants (e.g. shikimic acid pathway) phenylpropane compounds like the aromatic amino acids phenylalanine and tyrosine or lignin are depleted in ^{13}C relative to primary carbohydrates (cellulose) by 3–6 ‰ (Benner et al., 1987).

The very small depletion of the residues in ^{13}C above 340 °C indicates that isotope fractionation is of minor importance during thermal degradation at high temperatures. The temperature-dependent isotope fractionation processes, as measured in this study, were in contrast to measurements by Turekian et al. (1998) who found no differences in stable isotope composition between various combustion intensities expressed as fraction of OC converted to CO_2. However, more studies are necessary to understand stable carbon isotope fractionation during vegetation fires.

4.4. Effects of charring on organic structures

There were only small differences in the effects of charring on the NMR spectra of the hardwood and the softwood. Charring at 340 °C resulted in loss of the *O*-alkyl and di-*O*-alkyl structures that dominated the initial wood samples, and a large increase of aromatic carbon. There were also small increases in the intensity of the phenolic region and a broad alkyl signal comprised of methyl and short-chain alkyl substituents of the aromatic C. With increasing temperature, the aromatic character of the chars increased, as phenolic, C-substituted aromatic and alkyl structures decreased. Our NMR results follow the general trends seen in previous charring studies of cellulose (Pastorova et al., 1994; Sekiguchi et al., 1983), pectin (Sharma et al., 2001), wood (Solum et al., 1995; Baldock and Smernik, in press) and other lignocellulosic materials (Maroto-Valer et al., 1996; Freitas et al., 1999, 2001; Knicker et al., 1996), the results of course varying slightly with different combinations of time, temperature, sample particle size, and an inert vs. oxidizing atmosphere.

4.5. CP efficiency for chars

Low CP efficiency is typical of highly-condensed aromatic structures such as high-temperature biomass chars (Freitas et al., 1999, 2001; Maroto-Valer et al., 1996) and coke deposits (Fonseca et al., 1996; Maroto-Valer et al., 1998). Approximately 27% of the carbon was observed by CP for highly aromatic photooxidation residues of soil organic matter (Skjemstad et al., 1999). Similar results were obtained for wood chars prepared at 350 °C (36%, Smernik and Oades, 2000) and at 450 °C (29%, Baldock and Smernik, 2002), in both cases with correction for the effects of $T_{1\rho}{}^1H$ relaxation. We did not assess C observability by spin counting, as in those two studies, but CP efficiency was higher for the char samples in our study. The total integrated area of CP spectra was 0.42–0.49 of that observed for the corresponding BD spectra (i.e., CP enhancement was <0.5 compared to a theoretical maximum of 4). The discrepancy is even larger, as CP efficiency is reduced at high spinning speeds (Jakobsen et al., 1988), and the compensating ramped-amplitude technique (RAMP) was not available on our equipment (Preston, 2001). For three other chars derived from wood in wildfires, we found that CP efficiency at 8000 Hz was 0.57–0.73 of that at 4700 Hz (unpublished results).

There were only small differences in the alkyl vs. aromatic intensities obtained via CP or BD acquisition, especially for the 480 °C chars. As noted elsewhere, intensity distributions have to converge as aromaticities approach 100% (Maroto-Valer et al., 1996, 1998; Baldock and Smernik, in press). However, the underrepresentation of BC is more important in situations where it is associated with other carbon structures with higher CP efficiency, such as may occur in soil organic matter (Skjemstad et al., 1999; Smernik and Oades, 2000, Preston et al., 2002).

The DD spectra of our samples showed losses of 20–70% of aromatic intensity; for three out of four samples these are larger than the losses of ca. 15% expected for nonprotonated C (Fonseca et al., 1996), and were higher for the 480 °C chars. We also found high aromaticity in

the difference spectra showing protonated C. Apart from the shoulders due to phenolic and C-substituted C, the main aromatic peak is therefore likely due to a mixture of bridgehead C (shared by two or more aromatic rings), and protonated aromatic C with similar ranges of chemical shifts (Sullivan and Maciel, 1982; Netzel et al., 1996; Smernik and Oades, 2000; Solum et al., 2001).

The proportion of bridgehead vs. protonated aromatic C is determined by cluster size distribution, linkages, and the proportion of linear vs. cyclic condensation (Solum et al., 1995; Fonseca et al., 1996; Maroto-Valer et al., 1998). The higher DD losses, narrower aromatic peaks, and slightly higher CP efficiencies for the 480 °C chars are consistent evidence that loss of phenolic and alkyl substituents resulted in a relative increase of protonated aromatic C. This occurs as chars produced around this temperature form relatively small clusters of condensed C (including linear structures), that still have high proportions of protonated C (Solum et al., 1995). These carbons should be accessible by CP NMR, while those in the interior of condensed regions will only be detected by BD.

The low CP efficiency is thus likely due to a combination of remoteness from protons for carbon in condensed aromatic structures, plus reduction of $T_{1\rho}{}^{1}H$ values by organic free radicals in these same structures (Pastorova et al., 1994; Smernik and Oades, 2000; Preston, 2001; Baldock and Smernik, in press). The electrical conductivity (in ^{13}C NMR spectra seen as a downfield shift of the aromatic peak) and signal loss associated with graphitic structures are not found for chars produced from rigid biomass substrates at the relatively low temperatures of our study (Solum et al., 1995; Fonsesca et al., 1996; Freitas et al., 1999, 2001). It is also unlikely that paramagnetic cations play a large role, with fresh wood as a substrate, and a relatively low charring temperature.

5. Conclusions

Our study contributes to understanding molecular structural changes of organic carbon (OC) and black carbon (BC) formation during charring of wood in forest fires. We focused on the condition of smoldering combustion such as occurs in the inner part of burning logs. We investigated differences in charring and BC formation of soft- and hardwood representing coniferous and deciduous forests. As reported before, with increasing charring temperature, mass decreased and OC concentration increased. This study showed that charring at 150 °C led to an enrichment of ^{13}C in chars, probably due to the loss of lipids. Charring above 150 °C led to a depletion of ^{13}C in chars. At 340 °C the depletion was probably due to the dominant loss of cellulose and enrichment of lignin. At 480 °C the depletion could not be attributed to any specific constituent of the woods. ^{13}C MAS NMR revealed that OC composition of soft- and hardwood samples was dominated by *O*-alkyl and di-*O*-alkyl structures (holocellulose), and differed in the composition of phenolic and aromatic structures (lignin). With increasing temperatures, the molecular composition of OC of chars became similar and was dominated by aromatic structures (such as black carbon), with lower amounts of phenolic and alkyl carbon. With increasing temperature, the aromatic character of the chars increased, phenolic, C-substituted aromatic and alkyl structures decreased. Thus, temperature was the controlling factor in determining the qualitative composition of chars. However, initial differences in OC concentration and $\delta^{13}C$ value of soft- and hardwood were preserved during charring.

BC formed in this study (<500 °C) consisted mainly of relatively small clusters of condensed C, lacking a high proportion of bridgehead C, or graphitic characteristics.

The structure of BC formed here has two implications. First, the presence of small clusters may explain why levels of BC are low in ecosystems dominated by low-temperature smoldering fires when chemical methods are used which focus on highly condensed aromatic carbon structures. Second, small BC clusters are easier to oxidize than larger BC units and thus probably are less stable against degradation.

Associate Editor—**J.A. Rice**

Acknowledgements

We thank the working group of Willi A. Brand (Max-Planck-Institut fuer Biogeochemie, Jena, Germany) for measuring $\delta^{13}C$ and OC concentrations. We are grateful to the Studienstiftung des deutschen Volkes for financial support.

References

Amiro, B.D., Todd, J.B., Wotton, B.M., Logan, K.A., Flannigan, M.D., et al., 2001. Direct carbon emissions from Canadian forest fires, 1959–1999. Canadian Journal of Forest Research 31, 512–525.

Antal, M.J.J., Croiset, E., Dai, X., De Almeida, C., Shu-Lai Mok, W., et al., 1996. High-yield biomass charcoal. Energy and Fuels 10, 652–658.

Baldock, J.A., Smernik, R.J., 2002. Chemical composition and bioavailability of thermally altered *Pinus resinosa* (Red pine) wood. Organic Geochemistry 33, 1093–1109.

Banyasz, J.L., Li, S., Lyons-Hart, J., Shafer, K.H., 2001. Gas evolution and the mechanism of cellulose pyrolysis. Fuel 80, 1757–1763.

Benner, R., Fogel, M.L., Sprague, E.K., Hodson, R.E., 1987.

Depletion of ^{13}C in lignin and its implications for stable carbon isotope studies. Nature 329, 708–710.

Bird, M.I., Moyo, C., Veenendaal, E.M., Lloyd, J., Frost, P., 1999. Stability of elemental carbon in a savanna soil. Global Biogeochemical Cycles 13, 923–932.

Britt, P.F., Buchanan, A.C., Malcolm, E.A., 2000. Impact of restricted mass transport on pyrolysis pathways for aryl ether containing lignin model compounds. Energy and Fuels 14, 1314–1322.

Broadmeadow, M.S.J., Griffith, H., 1993. Carbon isotope discrimination and the coupling of CO_2 fluxes within forest canopies. In: Ehleringer, J.R., Hall, A.E., Farquhar, G.D. (Eds.), Carbon Isotope Discrimination and the Coupling of CO_2 Fluxes within Forest Canopies. Academic Press, San Diego, pp. 19–28.

Brugnoli, E., Scartazza, A., Lauteri, M., Monteverdi, M.C., Máguas, C., 1998. Carbon isotope discrimination in structural and non-structural carbohydrates in relation to productivity and adaptation to unfavourable conditions. In: Griffiths, H. (Ed.), Stable Isotopes Integration of Biological, Ecological and Geochemical Processes. BIOS Scientific Publishers, Oxford, pp. 133–146.

Davis, M.F., Schroeder, H.R., Maciel, G.E., 1994a. Solid-state ^{13}C nuclear magnetic resonance studies of wood decay. I. White rot decay of Colorado blue spruce. Holzforschung 48, 99–105.

Davis, M.F., Schroeder, H.R., Maciel, G.E., 1994b. Solid-state ^{13}C nuclear magnetic resonance studies of wood decay. II. White rot decay of paper birch. Holzforschung 48, 186–192.

Drysdale, D., 1999. An Introduction to Fire Dynamics. John Wiley & Sons, New York.

Ehleringer, J.R., Buchmann, N., Flanagan, L.B., 2000. Carbon isotope ratios in belowground carbon cycle processes. Ecological Applications 10, 412–422.

Elias, V.O., Simoneit, B.R.T., Cordeiro, R.C., Turco, B., 2001. Evaluating levoglucosan as an indicator of biomass burning in Carajás, Amazonia: a comparison to the charcoal record. Geochimica et Cosmochimica Acta 65, 267–272.

Falloon, P.D., Smith, P., 2000. Modelling refractory soil organic matter. Biology and Fertility of Soils 30, 388–398.

Fearnside, P.M., Graca, P.M.L.A., Rodrigues, F.J.A., 2001. Burning of Amazonian rainforest: burning efficiency and charcoal formation in forest cleared for cattle pasture near Manaus, Brazil. Forest Ecology and Management 146, 115–128.

Fonseca, A., Zeuthen, P., Nagy, J.B., 1996. ^{13}C n.m.r. quantitative analysis of catalyst carbon deposits. Fuel 75, 1363–1376.

Freitas, J.C.C., Bonagamba, T.J., Emmerich, F.G., 1999. ^{13}C high-resolution solid-state NMR study of peat carbonization. Energy and Fuels 13, 53–59.

Freitas, J.J.C., Bonagamba, T.J., Emmerich, F.G., 2001. Investigation of biomass-and polymer-based carbon materials using ^{13}C high-resolution solid-state NMR. Carbon 39, 535–545.

Glaser, B., Haumaier, L., Guggenberger, G., Zech, W., 2001. The ''Terra Preta'' phenomenon: a model for sustainable agriculture in the humid tropics. Naturwissenschaften 88, 37–41.

Gleixner, G., Czimczik, C.I., Kramer, C., Lühker, B., Schmidt, M.W.I., 2001. Plant compounds and their turnover and stabilization as soil organic matter. In: Schulze, E.-D., Heimann, M., Harrison, S., Holland, E., Lloyd, J., et al. (Eds.), Global Biogeochemical Cycles in the Climate System. Academic Press, San Diego, pp. 201–215.

Gleixner, G., Poirier, N., Bol, R., Balesdent, J., 2002. Molecular dynamics of organic matter in a cultivated soil. Organic Geochemistry 33, 357–366.

González-Vila, F.J., Tinoco, P., Almendros, G., Martin, F., 2001. Pyrolysis-GC-MS analysis of the formation and degradation stages of charred residues from lignocellulosic biomass. Journal of Agricultural and Food Chemistry 49, 1128–1131.

Harden, J.W., Trumbore, S.E., Stocks, B.J., Hirsch, A., Gower, S.T., et al., 2000. The role of fire in the boreal carbon budget. Global Change Biology 6, 1–11.

Hu, J.Z., Solum, M.S., Taylor, C.M.V., Pugmire, R.J., Grant, D.M., 2001. Structural determination in carbonaceous solids using advanced solid state NMR techniques. Energy and Fuels 15, 14–22.

Jakab, E., Faix, O., Till, F., 1997. Thermal decomposition of milled wood lignins studied by thermogravimetry/mass spectrometry. Journal of Analytical and Applied Pyrolysis 40- 41, 171–186.

Jakobsen, H.J., Daugaard, P., Langer, V., 1988. CP/MAS NMR at high speeds and high fields. Journal of Magnetic Resonance 76, 162–168.

Knicker, H., Almendros, G., González-Vila, F.J., Martín, F., Lüdemann, H.-D., 1996. ^{13}C- and ^{15}N-NMR spectroscopic examination of the transformation of organic nitrogen in plant biomass during thermal treatment. Soil Biology and Biochemistry 28, 1053–1060.

Kolodziejski, W., Frye, J.S., Maciel, G.E., 1982. Carbon-13 nuclear magnetic resonance spectrometry with cross polarization and magic-angle spinning for analysis of lodgepole pine wood. Analytical Chemistry 54, 1419–1424.

Kuhlbusch, T.A.J., 1995. Method for determining black carbon in residues of vegetation fires. Environmental Science & Technology 29, 2695–2702.

Kuhlbusch, T.A.J., 1998. Black carbon and the carbon-cycle. Science 280, 1903–1904.

Kuhlbusch, T.A.J., Andreae, M.O., Cachier, H., Goldammer, J.G., Lacaux, J.-P., et al., 1996. Black carbon formation by savanna fires: measurements and implications for the global carbon cycle. Journal of Geophysical Research 101, 23651–23665.

Kuhlbusch, T.A.J., Crutzen, P.J., 1995. Toward a global estimate of black carbon in residues of vegetation fires representing a sink of atmospheric CO_2 and a source of O_2. Global Biogeochemical Cycles 9, 491–501.

Mackay, D.M., Roberts, P.V., 1982. The dependence of char and carbon yield on lignocellulosic precursor composition. Carbon 20, 87–94.

Maroto-Valer, M.M., Andrésen, J.M., Rocha, J.D., Snape, C.E., 1996. Quantitative solid-state ^{13}C n.m.r. measurements on cokes, chars and coal tar pitch fractions. Fuel 75, 1721–1726.

Maroto-Valer, M.M., Atkinson, C.J., Willmers, R.R., Snape, C.E., 1998. Characterization of partially carbonized coals by solid-state ^{13}C NMR and optical microscopy. Energy and Fuels 12, 833–842.

McGraw, G.W., Hemingway, R.W., Ingram, L.L. Jr, Canady, C.S., McGraw, W.B.Thermal degradation of terpenes:

Camphene, Δ^3-carene, limonene, and α-terpinene. Environmental Science and Technology 33, 4029–4033.

Melzer, E., Schmidt, H.-L., 1987. Carbon isotope effects on the pyruvate dehydrogenase reaction and their importance for relative carbon-13 depletion in lipids. Journal of Biology & Chemistry 262, 8159–8164.

Mingle, J.G., Boubel, R.W., 1968. Proximate fuel analysis of some western wood and bark. Wood Science 1, 29–36.

Netzel, D.A., Miknis, F.P., Mitzel, J.M., Zhang, T., Jacobs, P.D., Haynes, H.W.J., 1996. Carbon-13 solid-state n.m.r. investigation of coke deposits on spent catalysts used in coal liquefaction. Fuel 75, 1397–1405.

Newman, R.H., Davies, L.M., Harris, P.J., 1996. Solid-state C-13 nuclear magnetic resonance characterization of cellulose in the cell walls of *Arabidopsis thaliana* leaves. Plant Physiology 111, 475–485.

O'Malley, V.P., Burke, R.A., Schlotzhauer, W.S., 1997. Using GC-MS/Combustion/IRMS to determine the $^{13}C/^{12}$ ratios of individual hydrocarbons produced from the combustion of biomass materials- application to biomass burning. Organic Geochemistry 27, 567–581.

Oren, M.J., Nassar, M.M., MacKay, G.D.M., 1984. Infrared study of inert carbonization of spruce wood lignin under helium atmosphere. Canadian Journal of Spectroscopy 29, 10–12.

Pastorova, I., Botto, R.E., Arisz, P.W., Boon, J.J., 1994. Cellulose char structure: a combined analytical Py-GC-MS, FTIR, and NMR study. Carbohydrate Research 262, 27–47.

Ponomarenko, E.V., Anderson, D.W., 2001. Importance of charred organic matter in Black Chernozem soils of Saskatchewan. Canadian Journal of Soil Science 81, 285–297.

Preston, C.M., 2001. Carbon-13 solid-state NMR of soil organic matter—using the technique effectively. Canadian Journal of Soil Science 81, 255–270.

Preston, C.M., Trofymow, J.A., Canadian Intersite Decomposition Experiment Working Group, 2000. Variability in litter quality and its relationship to litter decay in Canadian forests. Canadian Journal of Botany 78, 1269–1287.

Preston, C.M., Trofymow, J.A., Niu, J., Fyfe, C.A., 1998. ^{13}CPMAS-NMR spectroscopy and chemical analysis of coarse woody debris in coastal forests of Vancouver Island. Forest Ecology and Management 111, 61–68.

Preston, C.M., Trofymow, J.A., Niu, J., Fyfe, C.A., 2002. Harvesting and climate effects on organic matter characteristics in British Columbia coastal forests. Journal of Environmental Quality 31, 402–413.

Schleser, G.H., Frielingsdorf, J., Blair, A., 1999. Carbon isotope behaviour in wood and cellulose during artificial aging. Chemical Geology 158, 121–130.

Schmidt, M.W.I., Skjemstad, J.O., Gehrt, E., Kögel-Knabner, I., 1999. Charred organic carbon in German chernozemic soils. European Journal of Soil Science 50, 351–365.

Schmidt, M.W.I., Skjemstad, J.O., Czimczik, C.I., Glaser, B., Prentice, K.M., et al., 2001. Comparative analysis of black carbon in soils. Global Biogeochemical Cycles 15, 777–794.

Schmidt, W.I., Noack, A.G., 2000. Black carbon in soils and sediments: analysis, distribution, implications, and current challenges. Global Biogeochemical Cycles 14, 777–793.

Schnitzer, M., Hoffman, I., 1965. Thermogravimetry of soil humic compunds. Geochimica et Cosmochimica Acta 29, 859–870.

Schulze, E.-D., Lloyd, J., Kelliher, F.M., Wirth, C., Rebmann, C., et al., 1999. Productivity of forests in the Eurosiberian boreal region and their potential to act as a carbon sink—a synthesis. Global Change Biology 5, 1–20.

Sekiguchi, Y., Frye, J.S., Shafizadeh, F., 1983. Structure and formation of cellulosic chars. Journal of Applied Polymer Science 28, 3513–3525.

Shafizadeh, F., 1968. Pyrolysis and combustion of cellulosic materials. Advances in Carbohydrate Chemistry 23, 419–474.

Shafizadeh, F., 1982. Chemistry of pyrolysis and combustion of wood. In: Sarkanen, K.V., Tillman, D.A., Jahn, E.C. (Eds.), Chemistry of Pyrolysis and Combustion of Wood, vol. 3. Academic Press, San Diego, pp. 51–76.

Shafizadeh, F., Sekiguchi, Y., 1983. Development of aromaticity in cellulosic chars. Carbon 21, 511–516.

Sharma, R.K., Wooten, J.B., Baliga, V.L., Hajaligol, M.R., 2001. Characterization of chars from biomass-derived materials: pectin chars. Fuel 80, 1825–1836.

Skjemstad, J.O., Clarke, P.J., Taylor, A., Oades, J.M., McClure, S.G., 1996. The chemistry and nature of protected carbon in soil. Australian Journal of Soil Research 34, 251–271.

Skjemstad, J.O., Taylor, J.A., Smernik, R.J., 1999. Estimation of charcoal (char) in soils. Communications in Soil Science and Plant Analysis 30, 2283–2298.

Smernik, R.J., Oades, J.M., 2000. The use of spin counting for determining quantitation in solid-state ^{13}C NMR spectra of natural organic matter. 1. Model systems and the effects of paramagnetic impurities. Geoderma 96, 101–129.

Solum, M.S., Pugmire, R.J., Jagtoyen, M., Derbyshirre, F.Evolution of carbon structure in chemically activated wood. Carbon 33, 1247–1254.

Solum, M.S., Sarofim, A.F., Pugmire, R.J., Fletcher, T.H., Zhang, H., 2001. ^{13}C NMR analysis of soot produced from model compounds and a coal. Energy and Fuels 15, 961–971.

Sullivan, M.J., Maciel, G.E., 1982. Structural resolution in the carbon-13 nuclear magnetic resonance spectrometric analysis of coal by cross polarization and magic-angle spinning. Analytical Chemistry 54, 1606–1615. l.

Susott, R.A., 1980. Thermal behavior of conifer needle extractives. Forest Science 26, 347–360.

Susott, R.A., 1982. Characterization of the thermal properties of forest fuels by combustible gas analysis. Forest Science 28, 404–420.

Tinker, D.B., Knight, D.H., 2000. Coarse woody debris following fire and logging in Wyoming lodgepole pine forests. Ecosystems 3, 472–483.

Turekian, V.C., Ballentine, S.R.J., 1998. Garstang, M, Causes of bulk carbon and nitrogen isotopic fractionations in the products of vegetation burns: laboratory studies. Chemical Geology 152, 181–192.

Turunen, J., Tahvanainen, T., Tolonen, K., Pitkänen, A., 2001. Carbon accumulation in West Siberian mires, Russia. Global Biogeochemical Cycles 15, 285–296.

Völker, S., Rieckmann, T., 2002. Thermokinetic investigation of cellulose pyrolysis—impact of initial and final mass on kinetic results. Journal of Analytical and Applied Pyrolysis 62, 165–177.

Werner, R.A., Bruch, B.A., Brand, W.A., 1999. ConFlo III—an interface for high precision Δ^{13}C and Δ^{15}N analysis with

an extended dynamic range. Rapid Communications in Mass Spectrometry 13, 1237–1241.

Werner, R.A., Brand, W.A., 2001. Referencing strategies and techniques in stable isotope ratio analysis. Rapid Communications in Mass Spectrometry 15, 501–519.

Wiedemann, H.G., Riesen, R., Boller, A., Bayer, G., 1988. From wood to coal: a compositional thermogravimetric analysis. In: Earnest, C.M. (Ed.), From Wood to Coal: a Compositional Thermogravimetric Analysis. American Society for Testing and Materials, Philadelphia, pp. 227–244.

Wilson, M.A., Pugmire, R.J., Karas, J., Alemany, L.B., Woolfenden, W.R., et al., 1984. Carbon distribution in coals and coal macerals by cross polarization magic angle spinning carbon-13 nuclear magnetic resonance spectrometry. Analytical Chemistry 56, 933–943.